Article

Effect of PNA Backbone Modifications on Cyanine Dye Binding to PNA–DNA Duplexes Investigated by Optical Spectroscopy and Molecular Dynamics Simulations

Isil Dilek, Marcela Madrid, Rojendra Singh, Christian P. Urrea, and Bruce A. Armitage

J. Am. Chem. Soc., **2005**, 127 (10), 3339-3345• DOI: 10.1021/ja045145a • Publication Date (Web): 18 February 2005

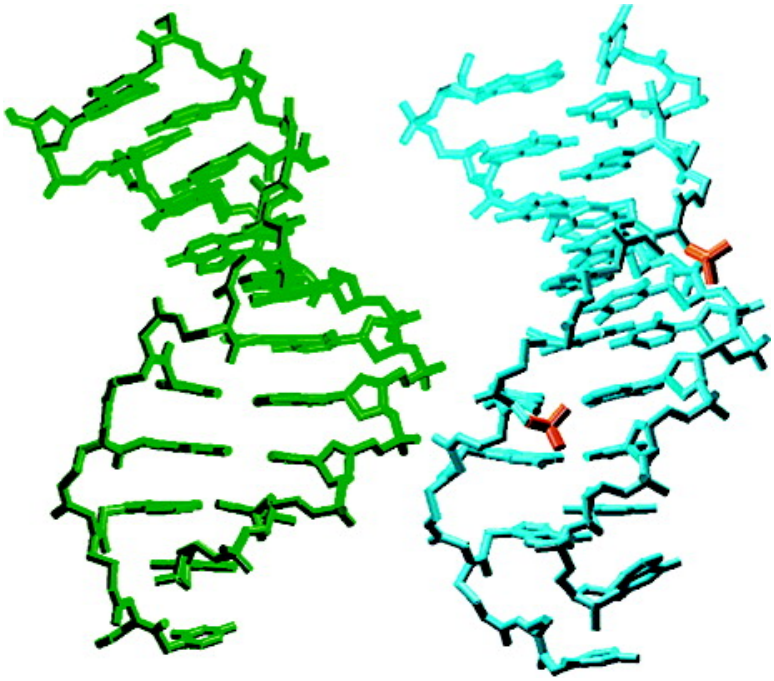

J|A|C|S
ARTICLES
Published on Web 02/18/2005

Effect of PNA Backbone Modifications on Cyanine Dye Binding to PNA−DNA Duplexes Investigated by Optical Spectroscopy and Molecular Dynamics Simulations

Isil Dilek,[†] Marcela Madrid,[‡] Rojendra Singh,[†] Christian P. Urrea,[†] and Bruce A. Armitage*,[†]

Contribution from the Pittsburgh Supercomputing Center and Department of Chemistry, Carnegie Mellon University, 4400 Fifth Avenue, Pittsburgh, Pennsylvania 15213

Received August 11, 2004; E-mail: army@andrew.cmu.edu

Abstract: Optical spectroscopy and molecular dynamics simulations have been used to study the interaction between a cationic cyanine dye and peptide nucleic acid (PNA)−DNA duplexes. This recognition event is important because it leads to a visible color change, signaling successful hybridization of PNA with a complementary DNA strand. We previously proposed that the dye recognized the minor groove of the duplex, using it as a template for the assembly of a helical aggregate. Consistent with this, we now report that addition of isobutyl groups to the PNA backbone hinders aggregation of the dye when the substituents project into the minor groove but have a weaker effect if directed out of the groove. UV−Visible and circular dichroic spectroscopy were used to compare aggregation on the different PNA−DNA duplexes, while molecular dynamics simulations were used to confirm that the substituents block the minor groove to varying degrees, depending on the configuration of the starting amino acid. In addition to a simple steric blockage effect of the substituent, the simulations suggest that directing the isobutyl group into the minor groove causes the groove to narrow and the duplex to become more rigid, structural perturbations that are relevant to the growing interest in backbone-modified PNA for applications in the biological and materials sciences.

Introduction

Peptide nucleic acid (PNA) is a synthetic DNA mimic in which the hydrogen-bonding nucleobases are attached to a polyamide backbone (Chart 1).[1−3] The lack of negative charges along the PNA backbone permits high-affinity hybridization to complementary DNA and RNA sequences,[4] even for targets that have competing secondary or tertiary structure.[5] This property has led to numerous studies and applications for PNA as an antisense agent, as a hybridization probe for diagnostics, and as a capture strand for purification of nucleic acids.[3,6]

The chemical structure of PNA leads to distinct helical secondary structures for its hybrids with DNA[7,8] and RNA.[9] The altered charge distribution along the backbone and distorted spatial distribution of hydrogen-bond donor and acceptor groups in the grooves of the helices relative to canonical DNA or RNA structures substantially impairs recognition by nucleic acid-binding proteins and small molecules. For example, Wittung et al.[10] found that the DNA intercalator ethidium bromide and minor-groove binder distamycin exhibited at least 100-fold lower affinity for PNA−DNA hybrids compared with homologous DNA−DNA duplexes. While several other methods are available for detecting PNA−DNA hybridization, a small-molecule ligand for reporting on PNA hybridization in solution would be useful for its simplicity.

In 1999, we reported the discovery of a group of cationic cyanine dyes that exhibited high-affinity, sequence-independent binding to PNA-containing hybrids such as PNA−DNA du-

Chart 1

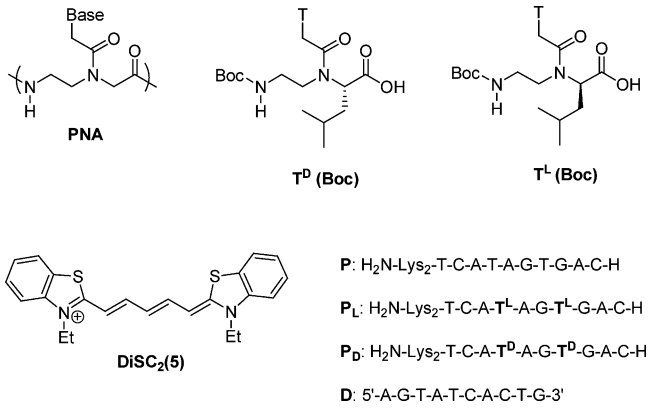

[†] Department of Chemistry.
[‡] Pittsburgh Supercomputing Center.

(1) Nielsen, P. E.; Egholm, M.; Berg, R. H.; Buchardt, O. *Science* **1991**, *254*, 1498−1500.
(2) Beck, F.; Nielsen, P. E. In *Artificial DNA: Methods and Applications*; Khudyakov, Y. E., Fields, H. A., Eds.; CRC Press: Boca Raton, FL, 2002; pp 91−114.
(3) Nielsen, P. E.; Egholm, M. In *Peptide Nucleic Acids: Protocols and Applications*, 2nd ed.; Nielsen, P. E., Ed.; Horizon Bioscience: Norfolk, VA, 2004; pp 1−36.
(4) Egholm, M.; Buchardt, O.; Christensen, L.; Behrens, C.; Freier, S. M.; Driver, D. A.; Berg, R. H.; Kim, S. K.; Nordén, B.; Nielsen, P. E. *Nature* **1993**, *365*, 566−568.
(5) Armitage, B. A. *Drug Discovery Today* **2003**, *8*, 222−228.
(6) Demidov, V. V. *Expert Rev. Mol. Diagn.* **2001**, *1*, 343−351.
(7) Leijon, M.; Graslund, A.; Nielsen, P. E.; Buchardt, O.; Nordén, B.; Kristensen, S. M.; Eriksson, M. *Biochemistry* **1994**, *33*, 9820−9825.
(8) Erikkson, M.; Nielsen, P. E. *Nat. Struct. Biol.* **1996**, *3*, 410−413.
(9) Brown, S. C.; Thomson, S. A.; Veal, J. M.; Davis, D. G. *Science* **1994**, *265*, 777−780.

plexes, PNA−PNA duplexes, and PNA_2−DNA triplexes.[11] In each case, the dye bound to the helix not as a monomer but rather as an aggregate, even under conditions where the dye was monomeric in solution. Thus, the PNA-containing double or triple helix acted as a template for the assembly of a helical cyanine dye aggregate. Of practical importance was the finding that these aggregates exhibit strongly blue-shifted absorption spectra, resulting in an instantaneous and visible color change from blue to purple, in the case of $DiSC_2(5)$ (Chart 1). This discovery has since been elaborated into assays for genetic screening and single nucleotide polymorphism detection.[12,13] While the relatively low sensitivity of this colorimetric response will likely preclude widespread applications, we have found the dye to be useful as a simple qualitative indicator for PNA hybridization to folded DNA target strands.[14,15]

The molecular-level details of the aggregation by cyanine dyes on PNA templates were not clearly determined in our previous work due to the lack of high-resolution structural information. The blue-shifted absorption band and exciton-coupled induced circular dichroic bands indicated that the dyes formed face-to-face H-aggregates with right-handed helicity. We speculated that the dyes were using the helical twist of the minor groove as the template for growth of the aggregate based on the fact that even in triple-helical hybrids, where the major groove is occupied by a second PNA strand, aggregation is unaffected. Nevertheless, the fact that aggregation seems to occur readily on any sequence indicates that if the minor groove is in fact the recognition site, then the dye molecules must not penetrate deeply into the groove, where sequence-dependent differences in the structure would be most significant.[16] To further test the hypothesis that the minor groove is involved in cyanine dye recognition of PNA hybrids, we synthesized PNA analogues with substituents that sterically block the minor groove. Circular dichroic spectropolarimetry, UV thermal melting curves, and molecular dynamics simulations demonstrate that these modified PNAs still form stable duplexes with their complementary DNA sequences, but UV−vis and CD spectra reveal that aggregation of the cyanine dye on these sterically blocked duplexes is significantly inhibited.

Experimental Section

Equipment. UV−vis measurements were performed on a Varian Cary3 spectrometer equipped with a thermoelectrically controlled multicell holder. CD measurements were recorded on a Jasco J715 spectropolarimeter equipped with a thermoelectrically controlled single cell holder.

UV Melting Curves. Samples including the appropriate amounts of complementary single strands of PNA and DNA were heated to 95 °C and equilibrated for 5 min. UV−vis absorbance at 260 nm was recorded every 0.5 °C as samples were cooled and then heated at a rate of 1.0 °C/min.

Dye Spectroscopic Experiments. PNA−DNA duplexes were prepared by mixing equimolar amounts of the complementary strands in buffer containing 100 mM NaCl, 10 mM sodium phosphate (pH 7.0), and 20% methanol, heating to 90 °C, and then cooling slowly (1 °C/min) to room temperature. Methanol was included in the buffer to minimize the adsorption of the dye/PNA complexes to the walls of the cuvettes. Samples were heated to 35 °C, and 1.0 μM aliquots of $DiSC_2$-(5) stock solution in methanol was added. The samples were cooled to 15 °C and allowed to equilibrate for 5 min before the UV−vis or CD spectrum was recorded. The samples were then heated to 35 °C prior to addition of the next aliquot.

Materials. Reagents and solvents were purchased from either Aldrich or Fisher Scientific and used without further purification. Boc-Leu-(D)·H_2O and Boc-Leu(L)·H_2O and di-*tert*-butyl dicarbonate were purchased from Peptides International; unmodified Boc-protected PNA monomers were from Applied Biosytems. DNA was purchased from Integrated DNA Technologies and used as received. DNA and PNA stock solutions were prepared in deionized water, and the concentrations were determined spectrophotometrically by use of extinction coefficients calculated from DNA nearest-neighbor values or PNA monomer values. $DiSC_2(5)$ was purchased from Aldrich and used without further purification. Stock solutions of the dye were prepared in methanol and filtered through glass wool. The concentration of $DiSC_2(5)$ was determined in methanol by use of the manufacturer's extinction coefficient ($\epsilon_{651} = 260\,000$).

PNA Oligomer Synthesis. PNA oligomers shown in Chart 1 were synthesized manually on a lysine-substituted MBHA resin by standard solid-phase peptide synthesis techniques.[17,18] Monomers were activated by HBTU for 1 min in the presence of MDCHA and pyridine to minimize racemization of chiral monomers during coupling. Oligomers were purified by reverse-phase high-performance liquid chromatography (HPLC) and characterized by matrix-assisted laser desorption ionization time-of-flight (MALDI-TOF) mass spectrometry (P, calculated mass 2985.99, observed mass 2986.81; P_L, calculated mass 3097.99, observed mass 3101; P_D, calculated mass 3097.99, observed mass 3096.05).

Molecular Dynamics Simulations. The PNA−DNA double helix was simulated by means of molecular dynamics as follows. The starting coordinates were obtained from the canonical B-DNA−DNA structure of the same sequence, simulated with the module nucgen of AMBER.[19] The DNA backbone and sugar atoms of one of the strands were substituted for their corresponding PNA atoms or deleted, according to the correspondence between the PNA and DNA backbone atoms.[20,21] Since this mapping scheme does not include the carbonyl oxygen atoms of the base linker, these atoms were added by geometrical calculation. The C7′−O7′ bonds were oriented toward the C-terminus of the PNA strand, as observed in NMR[8] and crystallographic[22] studies. The force field used was AMBER7 parm94,[23] complemented with previously determined parameters for the PNA backbone.[24] Hydrogen atoms and sodium ions were added with the module LEaP of AMBER.[19] The system was immersed in a water bath, where the minimum distance

(10) Wittung, P.; Kim, S. K.; Buchardt, O.; Nielsen, P. E.; Nordén, B. *Nucleic Acids Res.* **1994**, *22*, 5371−5377.
(11) Smith, J. O.; Olson, D. A.; Armitage, B. A. *J. Am. Chem. Soc.* **1999**, *121*, 2686−2695.
(12) Wilhelmsson, L. M.; Nordén, B.; Mukherjee, K.; Dulay, M. T.; Zare, R. N. *Nucleic Acids Res.* **2002**, *30*.
(13) Komiyama, M.; Ye, S.; Liang, X.; Yamamoto, Y.; Tomita, T.; Zhou, J.-M.; Aburatani, H. *J. Am. Chem. Soc.* **2003**, *125*, 3758−3762.
(14) Kushon, S. A.; Jordan, J. P.; Seifert, J. L.; Nielsen, P. E.; Nielsen, H.; Armitage, B. A. *J. Am. Chem. Soc.* **2001**, *123*, 10805−10813.
(15) Datta, B.; Armitage, B. A. *J. Am. Chem. Soc.* **2001**, *123*, 9612−9619.
(16) The same dye aggregates on certain DNA−DNA duplex templates by binding in the minor groove, but there is a strong sequence dependence and the aggregate structure is clearly different from the PNA-templated structures described here since the absorbance shifts to 590 nm for DNA−DNA compared with 530−540 nm for PNA−DNA. See Hannah, K. C.; Armitage, B. A. *Acc. Chem. Res.* **2004**, *37*, 845−853 for a review of DNA-templated cyanine dye aggregates.
(17) Christensen, L.; Fitzpatrick, R.; Gildea, B.; Petersen, K. H.; Hansen, H. F.; Koch, T.; Egholm, M.; Buchardt, O.; Nielsen, P. E.; Coull, J.; Berg, R. H. *J. Pept. Sci.* **1995**, *3*, 175−183.
(18) Koch, T. In *Peptide Nucleic Acids: Protocols and Applications*, 2nd ed.; Nielsen, P. E., Ed.; Horizon Bioscience: Norfolk, VA, 2004; pp 37−60.
(19) Pearlman, D. A.; Case, D. A.; Caldwell, J. W.; Ross, W. S.; Cheatham, T. E. I.; DeBolt, S.; Ferguson, D.; Seibel, G.; Kollman, P. *Comput. Phys. Commun.* **1995**, *91*, 1−42.
(20) Sen, S.; Nilsson, L. *J. Am. Chem. Soc.* **1998**, *120*, 619−631.
(21) Soliva, R.; Sherer, E.; Luque, F. J.; Laughton, C. A.; Orozco, M. *J. Am. Chem. Soc.* **2000**, *122*, 5997−6008.
(22) Rasmussen, H.; Kastrup, J. S.; Nielsen, J. N.; Nielsen, J. M.; Nielsen, P. E. *Nat. Struct. Biol.* **1997**, *4*, 98−101.
(23) Cornell, W. D.; Cieplak, P.; Bayly, C. I.; Gould, I. R.; Merz, K. M. J.; Ferguson, D. M.; Spellmeyer, D. C.; Fox, T.; Caldwell, J. W.; Kollman, P. A. *J. Am. Chem. Soc.* **1995**, *117*, 5179−5197.

from the surface of the double helix to the water box was 9 Å. Periodic boundary conditions and constant pressure and temperature were used. A 9 Å cutoff was used for the Lennard-Jones interactions. The particle mesh Ewald (PME)[25−27] method was used to treat the electrostatic interactions. The integration step was 1 fs, and SHAKE[28] was applied to constrain bonds involving hydrogen atoms. The nonbonded pair list was updated whenever an atom moved more than 0.5 Å since the last list update. First, the water was equilibrated by performing 5000 steps of energy minimization followed by 25 ps of molecular dynamics, while all PNA−DNA atoms were restrained with a force constant of 500 kcal/(mol·Å^2). Next, the temperature was raised to 300 K and the constraining force on the backbone atoms was slowly decreased to zero during 250 ps, while the bases were still constrained. Finally, the force constant on the bases was slowly decreased to zero during an additional 250 ps of molecular dynamics. All the atoms were then allowed to move. The structure obtained after 1.5 ns of molecular dynamics simulation was used to generate the two structures with leucine substitutions. Leu side chains replaced one of the hydrogens of the C5′ atoms of residues T14 and T17 of the PNA strand. The Leu side chains were both oriented toward the minor groove for one of the structures (P_LD) and away from the minor groove for the other structure (P_DD). Simulations for the three structures were continued for a total of 6.2 ns. The first 500 ps were not considered for the analysis, to ensure equilibration. Since we are interested in the effect of the Leu side chains in the minor groove, only the interval 0.5−4 ns was considered for the analysis of this trajectory. Helical parameters were measured with Curves,[29] and VMD was used for visualization.[30]

Results

Design. To block the minor groove of a PNA−DNA duplex, we decided to synthesize a backbone-modified PNA strand. The canonical PNA backbone consists of *N*-(2-aminoethyl)glycine units, but the α-carbon of the glycine component can be readily substituted by using other α-amino acids to synthesize the backbone. Numerous modifications of this type have been successfully introduced into PNA with only relatively minor decreases in affinity for complementary DNA strands.[31−35]

We chose to incorporate PNA monomers based on *N*-(2-aminoethyl)leucine because (i) L-leucine-modified PNA has already been shown to hybridize to complementary DNA with only modest destabilizations relative to unmodified PNA[33,34] and (ii) the uncharged isobutyl side chain should not directly affect the electrostatic contribution to aggregation of the cationic cyanine dye on the net anionic PNA−DNA duplex. On the basis of the NMR structure of a PNA−DNA duplex,[8] incorporation of leucine-based monomers having the L-configuration should result in projection of the isobutyl side chains toward the minor groove. On the other hand, the isobutyl side chains should point away from the minor groove when leucine-based monomers having the D-configuration are incorporated into the PNA strands. Thus, L-leucine-modified PNA would be expected to inhibit cyanine dye aggregation to a greater degree than would a D-leucine-modified analogue.

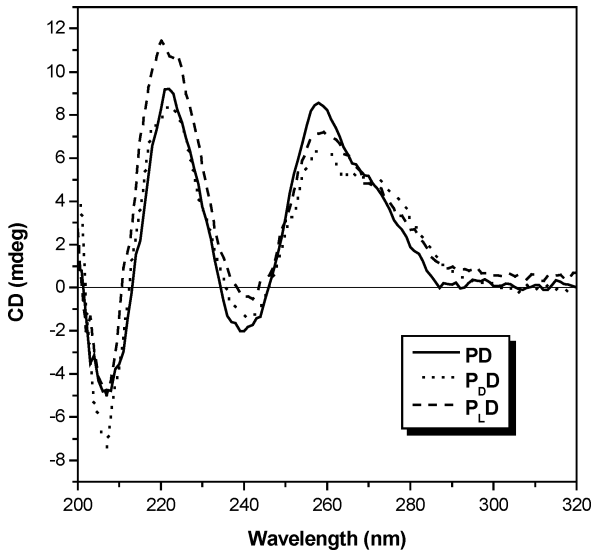

Figure 1. Circular dichroic spectra recorded for 5.0 μM unmodified (PD) and modified (P_LD and P_DD) PNA−DNA duplexes. Samples were prepared in 10 mM sodium phosphate buffer (pH = 7.0) with 100 mM NaCl and 20% methanol. Spectra were recorded at 25 °C, and eight scans collected at 100 nm/min were averaged.

Synthesis and Characterization of Modified PNA−DNA Templates. Details of the synthesis of modified PNA monomers constructed from L- and D-leucine with thymine as the nucleobase are given in the Supporting Information and follow the approach used by Haaima et al.[32] with only minor modification. These monomers were then incorporated into PNA decamers P_L and P_D at two positions (Chart 1; T^L and T^D represent the T monomers constructed from L- and D-leucine, respectively). An unmodified PNA strand (P) was also synthesized for comparison. Two L-lysine amino acids were included at the C-terminus of the PNA strands to provide water solubility. PNA oligomers were synthesized manually by standard solid-phase peptide synthetic techniques,[17,18] purified by HPLC, and characterized by MALDI-TOF mass spectrometry.

Hybridization of PNA single strands with complementary DNA strands yields double-helical structures, which can be characterized by circular dichroic (CD) spectropolarimetry and UV melting studies.[4] Figure 1 presents CD spectra recorded for 5 μM PD, P_DD, and P_LD duplexes. CD spectra for all three duplexes are very similar and match previously reported spectra for PNA−DNA double-helical structures. It is clear that incorporation of L- and D-leucine-modified PNA monomers does not alter the gross structural features of the hybrid, although the variation in intensity may signal minor local changes in the helical structure.

Denaturation of a duplex to its component single strands usually results in a substantial increase in the absorbance at 260 nm (hyperchromicity) due to unstacking of the bases. The midpoint of this transition is referred to as the T_m (melting point) of the duplex. Figure 2 shows the denaturation curves for the unmodified PNA−DNA duplex (PD) as well as L-leucine (P_LD)

(24) Shields, G. C.; Laughton, C. A.; Orozco, M. *J. Am. Chem. Soc.* **1998**, *120*, 5895−5904.
(25) Darden, T.; York, D.; Pedersen, L. *J. Chem. Phys.* **1993**, *98*, 10089−10092.
(26) Darden, T. A.; Bartolotti, L.; Pedersen, L. G. *Environ. Health Perspect. Suppl.* **1996**, *104*, 69−74.
(27) Essmann, U.; Perera, L.; Berkowitz, M. L.; Darden, T.; Lee, H.; Pedersen, L. G. *J. Chem. Phys.* **1995**, *103*, 8577−8593.
(28) van Gunsteren, W. F.; Berendsen, H. J. C. *Mol. Phys.* **1997**, *34*, 1311−1327.
(29) Lavery, R.; Sklenar, H. Curves 5.1, Computer Program; Institut de Biologie Physico-Chimique, CNRS, 1996.
(30) Humphrey, W.; Dalke, A.; Schulten, K. *J. Mol. Graphics* **1996**, *14*, 33−38.
(31) Dueholm, K. L.; Petersen, K. H.; Jensen, D. K.; Egholm, M.; Nielsen, P. E.; Buchardt, O. *Bioorg. Med. Chem. Lett.* **1994**, *4*, 1077−1080.
(32) Haaima, G.; Lohse, A.; Buchardt, O.; Nielsen, P. E. *Angew. Chem., Int. Ed. Engl.* **1996**, *35*, 1939−1942.
(33) Püschl, A.; Sforza, S.; Haaima, G.; Dahl, O.; Nielsen, P. E. *Tetrahedron Lett.* **1998**, *39*, 4707−4710.
(34) Sforza, S.; Haaima, G.; Marchelli, R.; Nielsen, P. E. *Eur. J. Org. Chem.* **1999**, 197−204.
(35) Sforza, S.; Corradini, R.; Ghirardi, S.; Dossena, A.; Marchelli, R. *Eur. J. Org. Chem.* **2000**, 2905−2913.

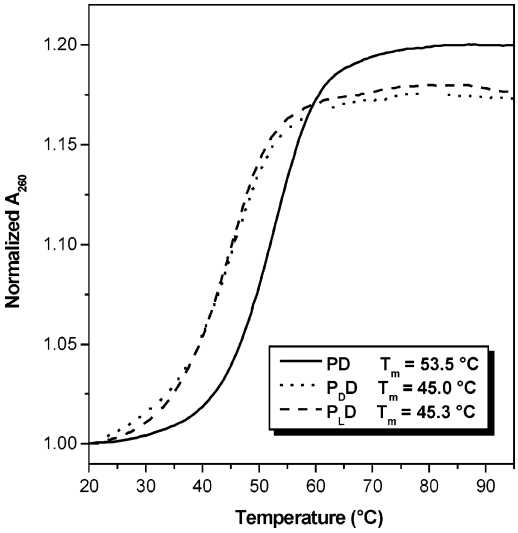

Figure 2. UV melting curves of 5.0 μM PNA−DNA duplexes. Data were collected at 0.5 °C intervals during a heating ramp of 1.0 °C/min.

Table 1. Comparison of the Helicoidal Parameters of the Three Averaged Structures, an NMR-Determined PNA−DNA,[8] and Canonical B-DNA[a]

	global avg twist (deg)	diameter (Å)	pitch (Å)
PD	28	21	42
P_LD	32	18	39
P_DD	25	21	54
NMR	28	22	42
canonical B-DNA	36	15	34

[a] Determined at the C5′ atoms of each base pair with Curves.[29]

and D-leucine (P_DD) modified analogues. Incorporation of leucine side chains decreases the melting temperature of the PNA−DNA duplex by ca. 4 °C/modified residue, regardless of the chirality. Similar results for modified PNAs were reported previously by Nielsen and co-workers.[32] Importantly, the modified duplexes are fully formed at the temperatures and concentrations used for the spectroscopic experiments described below.

Molecular Dynamics Simulations. Molecular dynamics simulations were performed to further evaluate the structure of the three duplexes. In each case, the PNA−DNA duplex was constructed from a canonical B-form duplex as described in the Experimental Section. The helical structure departed quickly from the starting B-form geometry, with a root-mean-square (RMS) deviation between the PNA−DNA structure and canonical B-DNA, averaged over the last 2 ns of the simulation, of 5.3 Å. This is in agreement with previous molecular dynamics simulations, which obtained RMS deviations between PNA−DNA double helices and B-DNA of 4−5 Å.[21] The three simulated structures remain double-helical and stable during the trajectories, as indicated by stable RMS and energetic values.

Table 1 lists the helical parameters for the three duplexes, along with those determined from a solution NMR structure of an unmodified PNA−DNA duplex.[8] The parameters for B-form DNA are also included for comparison. The simulations effectively reproduce the NMR parameters for the unmodified duplex. For the L-leucine-modified PNA, the twist increases, leading to a decrease in helical pitch, while the opposite is observed for the D-leucine-modified analogue.

Differences between the two leucine-modified structures are also evident when the minor-groove widths of the duplexes are

Table 2. Minor-Groove Widths[a] of the Simulated Structures, Averaged over the Trajectories

base pair	PD	P_LD	P_DD
A_1-T_{20}	7		8
G_2-C_{19}	6	6	6
T_3-A_{18}	6	4	8
A_4-T_{17}	**7**	**4**	**9**
T_5-A_{16}	8	4	8
C_6-G_{15}	8	4	8
A_7-T_{14}	**8**	**5**	**7**
C_8-G_{13}	7	5	6
T_9-A_{12}	5	6	7
G_{10}-C_{11}[b]			

[a] Determined at the C5′ atoms of each base pair with Curves[29] and given in angstroms. Positions of leucine modification are shown in boldface type. [b] The minor-groove width was undefined for this base pair.

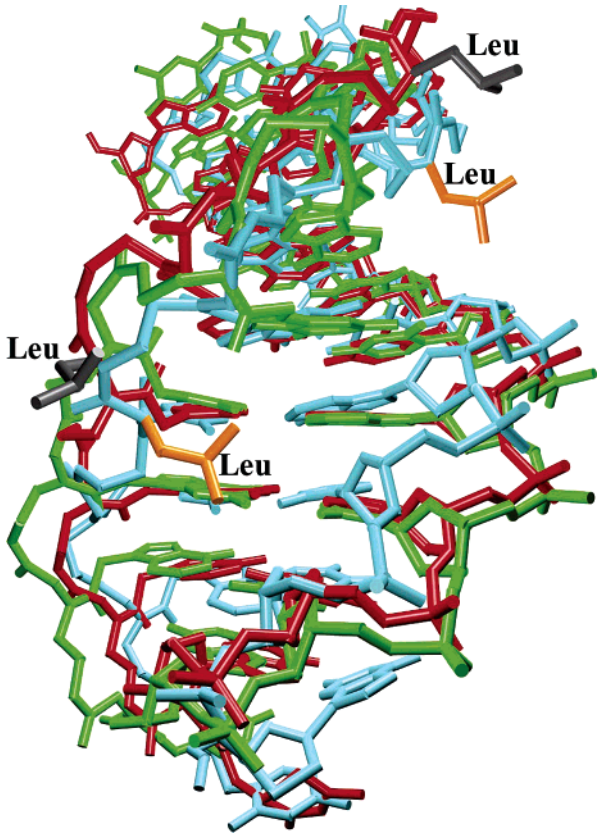

Figure 3. View into the minor groove of the three simulated duplex structures, unmodified PD (green), P_LD (blue), and P_DD (red). Structures are averaged over the trajectories. The leucine side chains are labeled and colored orange (L-configuration, directed into the minor groove) and gray (D-configuration, directed away from the minor groove).

measured at each base pair (Table 2). When the isobutyl substituents are directed toward the minor groove, the effect is to make the minor groove narrower than in the unmodified duplex by up to 50%. The narrowing is most pronounced at the center of the duplex, i.e., closest to the two modifications. In contrast, the D-leucine modifications have virtually no effect on the minor-groove width. No significant effect on the major-groove widths was observed in the simulated structures (data not shown).

Superposed views into the minor grooves for the three structures are shown in Figure 3. The gross similarities in the three helices are consistent with the lack of significant variation in the CD spectra. As designed, the L-leucine side chains (orange) project directly into the minor groove while the

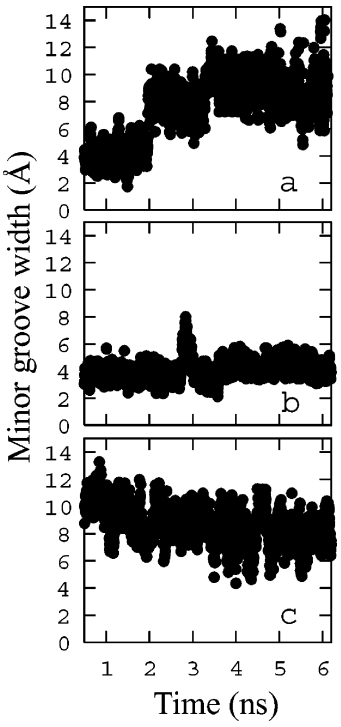

Figure 4. Minor-groove widths measured between the C5′ atoms of base pair A4-T17 as a function of time for (a) PD, (b) P_LD, and (c) P_DD.

D-leucine side chains (gray) are directed into solution. The narrowed minor groove for the L-leucine-modified duplex is also evident in the figure. Interestingly, the structural perturbation involves not only the PNA strand but also the DNA strand (compare the blue structure with the red and green ones).

An additional interesting feature of the simulations arose from plotting the minor-groove widths at one of the modification sites as a function of time (Figure 4). The trajectories are stable over the last 3 ns of the simulation and the narrower groove for P_LD is evident, but what is striking about the data is the significantly smaller fluctuations in the groove width for this duplex. This suggests that the L-leucine modifications *increase* the rigidity of the duplex while the D-leucine modification has no effect.

Assembly of Cyanine Dye Aggregates. Aggregation of cyanine dyes on PNA−DNA templates is readily monitored by optical spectroscopy.[11,37] Both UV−vis and circular dichroic (CD) spectra show blue-shifted bands not observed in the absence of the PNA−DNA duplex. This effect is illustrated in the UV−vis spectra of Figure 5A, where increasing amounts of the dicarbocyanine dye $DiSC_2(5)$ are added into a solution of 5 μM PD. The new absorption band at 543 nm is diagnostic for successful aggregation of the dye on the template. At low dye concentrations, the absorption spectrum is similar to the absorption spectrum of the dye in methanol. At higher dye concentrations, the new peak at 543 nm is prominent. We previously attributed this concentration dependence to the high stoichiometry ($\geq$6 dyes/duplex) and cooperative nature of the aggregation process.[11]

Introduction of two L-leucine modifications into the PNA strand significantly hinders aggregation of the dye (Figure 5B). While the aggregate peak at 543 nm is quite strong for the PD, this feature appears only as a weak shoulder at even the highest dye/duplex ratio when P_LD is used as the template. $DiSC_2(5)$ forms noncovalent dimers in aqueous solution and exhibits an absorption band at 579 nm.[37] The band at 579 nm in Figure 5B indicates that as the $DiSC_2(5)$ concentration increases, the dye dimerizes in solution rather than aggregating on the template. Conversely, the absence of this band in Figure 5A illustrates the preferential aggregation of the dye on the unmodified PD template. Clearly, the presence of two T^L monomers prevents the aggregation of the dye on P_LD.

As expected, $DiSC_2(5)$ shows markedly better aggregation on the D-leucine-modified template (P_DD). UV−Vis spectra for the dye in the presence of the three templates are shown in Figure 6. The stronger absorption band at 543 nm for P_DD compared to P_LD is consistent with the MD simulations, which indicated that the D-leucine substituents project away from the minor groove. Nevertheless, the weaker absorption for P_DD relative to the unmodified duplex indicates that the D-leucine modifications do impair binding of the dye.

Analogous dye binding experiments were performed by CD. $DiSC_2(5)$ is achiral, so the unbound dye in solution does not present any CD signal. When it binds to PNA-containing hybrids and assembles into helical aggregates, it exhibits a strong induced CD signal.[11] This phenomenon is demonstrated in Figure 7. Binding of $DiSC_2(5)$ to PD induces a strong positive CD signal at 552 nm and a negative signal at 521 nm. The bisignate bands are attributed to exciton coupling due to the interaction of two or more neighboring chromophores,[38] indicating the aggregation of multiple dye molecules on the PD template. In addition, the positive splitting provides evidence of a right-handed helical relationship for the dye chromophores, consistent with templating of the aggregate by the PNA−DNA duplex, which is itself a right-handed helix. In contrast, the CD signal for P_LD is 5−6-fold weaker, consistent with the UV−vis results. In addition, the lack of a CD signal in the region of 579 nm verifies that the UV−vis maximum observed at this wavelength for P_LD is due to *unbound*, dimerized dye. As with the UV−vis experiment, the induced CD signal for $DiSC_2(5)$ in the presence of P_DD is intermediate between the other two templates.

Figure 8 illustrates the dye concentration dependence for aggregation on the three PNA−DNA templates as measured by the intensity of the negative CD band. The results further illustrate the differential impact of the two leucine configurations on dye aggregation: L-leucine modifications hinder dye aggregation to a much greater extent than do D-leucine modifications.

Finally, we previously described how the cooperative nature of dye aggregation on PNA−DNA leads to highly temperature-dependent binding, reflected in "melting" transitions for the aggregates that are independent of those for the templates.[11,36] Figure 9 shows melting curves for $DiSC_2(5)$ on the three templates recorded by the UV−vis absorbance at 543 nm. The L-leucine-modified template reduces the stability of the aggregate by 8.8 °C, compared with only 4.8 °C for the D-analogue. The reductions in melting temperature reflect the fact that less dye is bound to the two modified templates based on the intensity of the dye monomer absorption band in Figure

(36) Wang, M.; Dilek, I.; Armitage, B. A. *Langmuir* **2003**, *19*, 6449−6455.
(37) West, W.; Pearce, S. *J. Phys. Chem.* **1965**, *69*, 1894−1903.
(38) Nakanishi, K.; Berova, N.; Woody, R. W. *Circular Dichroism: Principles and Applications*; VCH Publishers: New York, 1994.

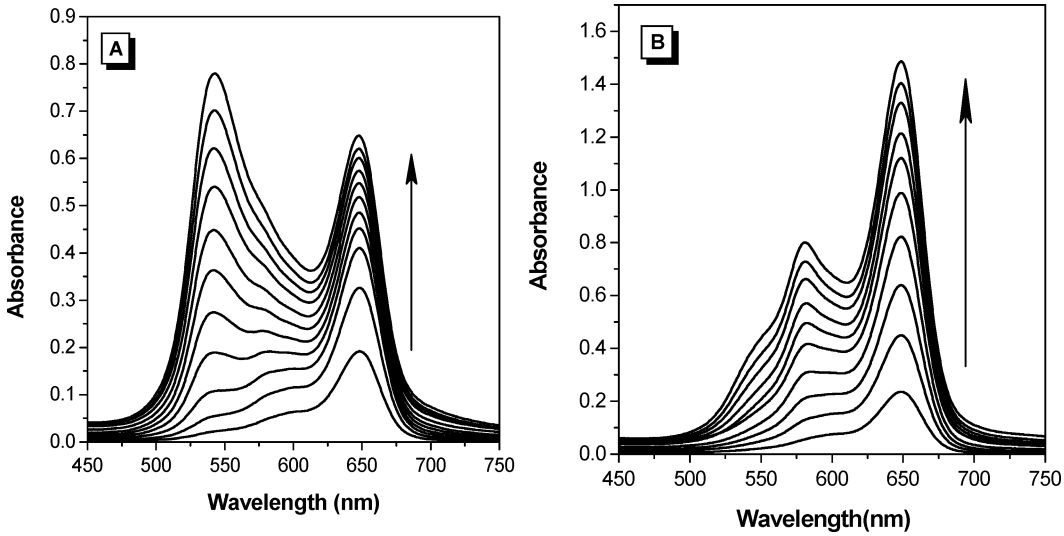

Figure 5. UV−Vis titration of $DiSC_2(5)$ into (A) PD or (B) P_LD template duplexes. [PNA−DNA] = 5.0 μM; dye was added in 1.0 μM aliquots. Spectra were recorded at 15 °C.

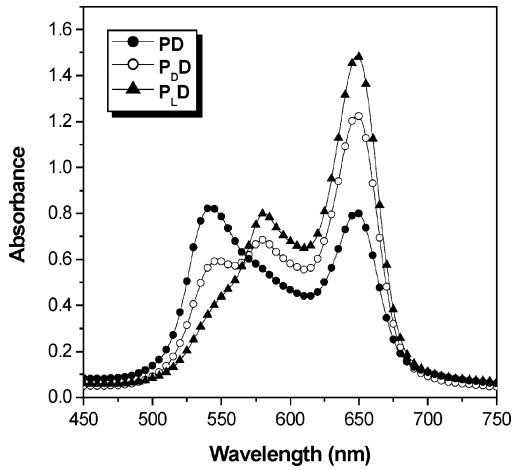

Figure 6. Comparison of UV−vis spectra recorded for $DiSC_2(5)$ in the presence of the three PNA−DNA duplexes. [PNA−DNA] = 5.0 μM; [$DiSC_2(5)$] = 10 μM. Spectra were recorded at 15 °C.

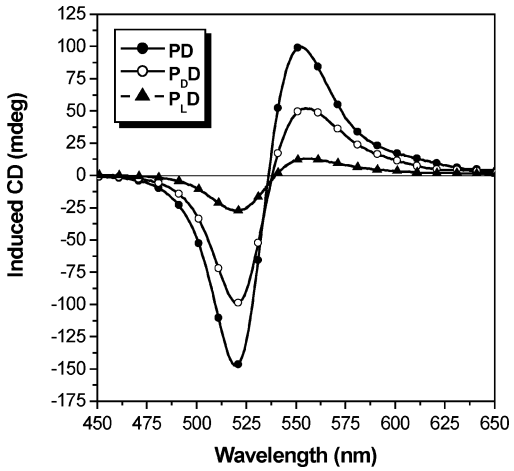

Figure 7. Comparison of CD spectra recorded for $DiSC_2(5)$ in the presence of the three PNA−DNA duplexes. [PNA−DNA] = 5.0 μM; [$DiSC_2(5)$] = 10 μM. Four scans were collected at a scan rate of 200 nm/min and averaged. Spectra were recorded at 15 °C.

6. Our previous work showed that the stability of the aggregate is strongly dependent on the dye concentration.[11]

Discussion

To test our earlier conjecture that $DiSC_2(5)$ uses the minor groove of PNA-containing duplexes and triplexes as a template for assembling a dye aggregate, we synthesized PNA oligomers based on chiral monomers that project alkyl groups either into or out of the minor groove. The leucine side chains we incorporated introduced thermal destabilizations of 4.1−4.2 °C/modification relative to a glycine-based PNA, independent of the configuration. It is difficult to compare this with other results in the literature, since different sequences, numbers, and positions of modifications and terminal charges were used. However, while the destabilizations we observe in this work are larger than those reported previously, the P_LD and P_DD duplexes are fully formed at the temperatures at which dye-binding experiments were performed.

The UV−vis and CD results described above clearly demonstrate that incorporation of L-leucine-derived PNA monomers into a PNA−DNA duplex significantly hinders cyanine dye aggregation, whereas the D-leucine analogue is less inhibitory. Interestingly, the molecular dynamics simulations suggest that the effect of the isobutyl group is not only to block access to the groove but also to induce changes in both the width and the rigidity of the groove. In addition to our earlier report that blockage of the major groove by use of a second PNA strand to form a PNA_2−DNA triplex has almost no effect on dye aggregation, these results provide further evidence that the dye molecules aggregate by using the minor groove of the PNA−DNA double helix as a template.

The fact that aggregation on the D-leucine-derived template is not restored to that of the unmodified duplex could be due to several factors, including differential hydration of the unmodified and D-leucine-derived duplexes, residual steric blockage by the isobutyl group even in the D-configuration, or a local change in the helical geometry. The altered helical parameters obtained from the MD simulations for P_DD versus PD (Table 1) are consistent with the last option. An additional factor to consider is the possibility of racemization of the chiral PNA monomer during synthesis. Corradini, Nielsen, and co-workers[39,40] recently reported a systematic study of racemization in which they varied the conditions for forming the active ester

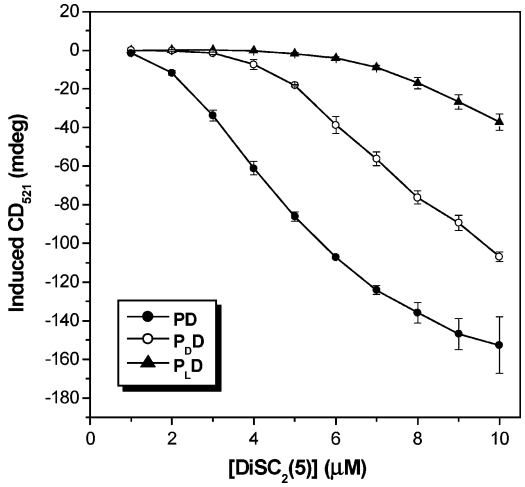

Figure 8. Plot of the induced CD intensity at 521 nm as a function of $DiSC_2(5)$ concentration in the presence of PD, P_DD, and P_LD (5.0 μM). Data points and error bars represent the mean and standard deviation of three separate experiments.

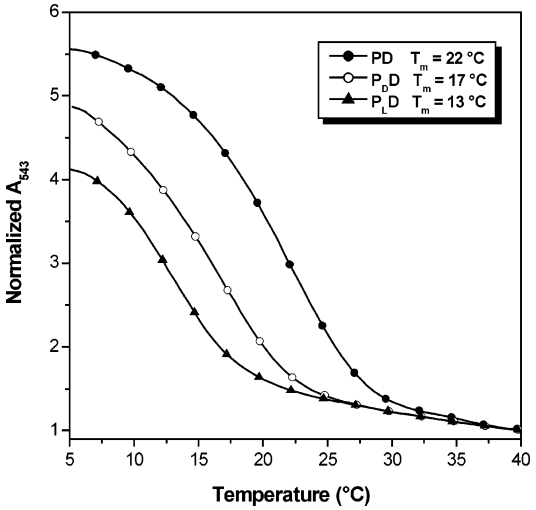

Figure 9. Temperature-dependent absorbance curves recorded at 543 nm for $DiSC_2(5)$ (10 μM) in the presence of PD, P_DD, and P_LD (5.0 μM). Cooling curves were collected from 40 to 5 °C at a rate of 0.5 °C/min.

prior to coupling of the chiral monomer onto the growing PNA oligomer. While leucine-modified monomers were not investigated, a phenylalanine-derived monomer underwent 5−6% racemization under conditions similar to what we used for our couplings. Thus, we estimate that our PNA strands are approximately 90% either L,L- or D,D-configuration. The presence of a minor amount of L-leucine-containing PNA in the otherwise D,D-configuration duplexes would account at least in part for the inability to restore dye aggregation to the level observed on the unmodified template.

In conclusion, the experiments reported here are consistent with a molecular recognition mechanism in which cyanine dyes assemble into helical aggregates by using the minor groove of a PNA−DNA duplex as a template. This is distinct from minor-groove recognition of duplex DNA in that the dyes most likely do not penetrate to the floor of the groove, where sequence-dependent structural features would be most evident. Rather, in this model the dyes are bound rather loosely by the groove, as evidenced by the relatively low temperatures required to dissociate the aggregate.

Acknowledgment. This work was supported by grants from Research Corporation and the National Science Foundation (CHE-0315925) to B.A.A. M.M. thanks M. Orozco and R. Soliva for sharing their PNA parameters. All simulations were performed on the Terascale System at the Pittsburgh Supercomputing Center supported by NSF CHE-020022. Mass spectra were measured in the Center for Molecular Analysis at Carnegie Mellon University, supported by NSF CHE-9808188.

Supporting Information Available: Experimental details of chiral PNA monomer synthesis (PDF). This information is available free of charge via the Internet at http://pubs.acs.org.

JA045145A

(39) Tedeschi, T.; Corradini, R.; Marchelli, R.; Pushl, A.; Nielsen, P. E. *Tetrahedron: Asymmetry* **2002**, *13*, 1629−1636.
(40) A recently reported submonomeric strategy for synthesizing PNAs with chiral backbones affords significantly improved optical purity: Sforza, S.; Tedeschi, T.; Corradini, R.; Ciavardelli, D.; Dossena, A.; Marchelli, R. *Eur. J. Org. Chem.* **2003**, 1056−1063.